

# First-order phase transition and the equation of state in a 2D granular fluid

M. D. Shattuck\*

*Benjamin Levich Institute and Physics Department,  
The City College of the City University of New York 140th and Convent Ave., New York, NY 10031  
(Dated: March 23, 2022)*

We present experimental evidence for a first-order freezing/melting phase transition in a nonequilibrium system — an oscillated two-dimensional isobaric granular fluid. The steady-state transition occurs between a gas and a crystal and is characterized by a discontinuous change in both density and temperature. It is suppressed if the number of particles is incommensurate with the cell size, shows rate-dependent hysteresis, and obeys the Lindemann criterion for melting. Further, the measured equation of state both above and below the phase transition compares well with theory.

PACS numbers: 45.70.-n, 51.30.+j, 51.10.+y, 64.70.Hz

*Introduction:* Granular materials are fascinating systems, which have tremendous technological importance and numerous applications to natural systems. They also represent a serious challenge to statistical physics as an extreme example of a system far from equilibrium. As for any macroscopic system, the total number of modes in a collection of grains is on the order of Avogadro's number  $N_A$ . However, in granular systems a very small number of modes, specifically the translational and rotational mode of the  $N$  macroscopic grains which make up the system, can be preferentially excited by external forces like moving walls. The energy in these  $\sim N$  modes can be many orders of magnitude above the average energy per mode (i.e., the temperature) for the remaining  $N_A$  modes. The study of the relaxation of this extremely far-from-equilibrium system toward equilibrium is the challenge of granular statistical mechanics. In this paper, we experimentally examine the nonequilibrium steady-state (NESS) created by a balance between relaxation (dissipation) and injection of energy (heating), and specifically, a first-order melting/freezing phase transition and the equation of state in a two-dimensional (2D) inelastic hard sphere system heated (excited) from below under isobaric conditions.

The elastic hard sphere system is the simplest system which undergoes a first-order phase transition [1, 2]. This transition has been seen in simulation [3] and experiments in colloids [4]. However, in these systems energy is conserved, and the concept of free energy is well defined. In dissipative systems, such as inelastic hard spheres or granular systems, the concept of free energy is not established [5], even in a NESS, since there is a constant flow of energy through the system. The idea of applying thermodynamics to a NESS is at the forefront of current statistical physics [6]. The demonstration of experimental systems which undergo first-order phase transitions under NESS conditions points to the universality of entropy-production and free-energy concepts even in the absence of energy conservation.

*Experiment:* We place  $N$  (26–85) spherical stainless steel ball bearings of diameter  $D = 3.175$  mm in a con-

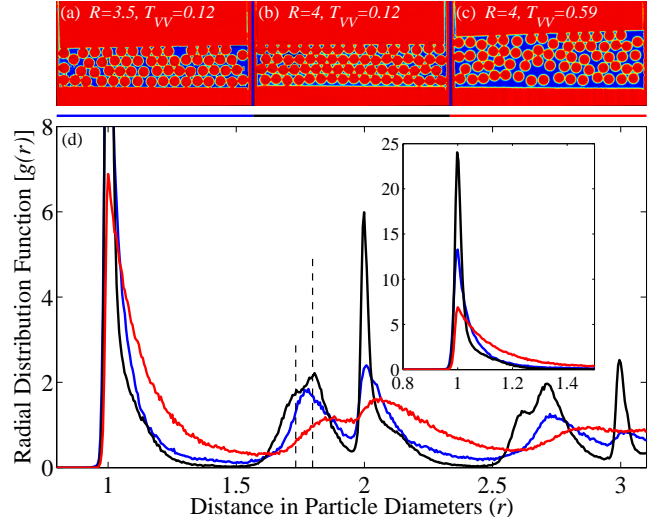


FIG. 1: (a)-(c) Photographs of a 2D granular layer, with freely floating (isobaric) weight: (a)  $R = 3.5$ ,  $\Gamma = 3.88$ ,  $T_{VV} = 0.12$ , disordered with crystalline regions. (b)  $R = 4$ ,  $\Gamma = 7.90$ ,  $T_{VV} = 0.12$ , crystal. (c)  $R = 4$ ,  $\Gamma = 8.10$ ,  $T_{VV} = 0.59$ , gas. (d) The radial distribution function for states (a)-(c). The line style is indicated below each image. The vertical lines show next-nearest-neighbor distances. The short line is  $\sqrt{3}D$  and the long line is  $\sqrt{3}$  times the average nearest-neighbor distance in (b). The inset shows the first peak at full scale.

tainer  $17.5 D$  wide by  $20 D$  tall by  $1 D$  deep as shown in Fig. 1(a-c). We define the number of rows  $R = N/17$ , where 17 is the number of particles to fill an entire row. A thin plunger slides through a slot in the bottom of the cell and oscillates sinusoidally to excite (heat) the particles from below. The driving is characterized by the nondimensional maximum acceleration  $\Gamma = A(2\pi f)^2/g$ , where  $A$  is the maximum amplitude of the plunger,  $f$  is the frequency and  $g$  is the acceleration of gravity. A freely floating weight confines the particles from the top, allowing the volume to fluctuate but providing constant pressure conditions. When  $\Gamma$  is large the granular system acts like a gas, as shown in Fig. 1(c). When  $\Gamma$  is small and  $R$  is an integer a crystalline state develops [see Fig.

1(b)]. Using high-speed digital photography we measure the positions of the plunger, the weight, and all of the particles in the cell with a relative accuracy of 0.2% of  $D$  or approximately  $6\mu\text{m}$  at a rate of 840 Hz. We track the particles from frame to frame and assign a velocity to each one, typically  $\sim D/5$  per frame.

From these data we measure the volume, density, and granular temperature or average kinetic energy per particle. In a normal gas, the temperature is isotropic and the kinetic energy in vertical velocity is the same as that in horizontal velocity. In a granular system, due to dissipation, at least two temperatures are needed in two dimensions, a horizontal temperature  $T_{HH} = 1/2m\langle(v_x - \langle v_x \rangle)^2\rangle$  and a vertical temperature  $T_{VV} = 1/2m\langle(v_y - \langle v_y \rangle)^2\rangle$ , where  $m$  is the mass of the particles and  $v_x$  and  $v_y$  are the horizontal and vertical velocities respectively. We want to assign a single value to each temperature, so we take the averages over all particles and time ( $\sim 50$  periods). The most obvious implementation of the averages  $\langle \dots \rangle$  is in the inertial lab frame; however, this produces a finite temperature even if the plunger, particles, and weight all move with the same velocity. Taking the averages in the center of mass frame of the particles solves this problem, but the velocities are no longer simply related to the collision velocities with the weight used in the derivation of the equation of state. We have chosen to evaluate the averages in the frame of the weight. This choice solves both problems. The ultimate solution is to allow the temperature, density, and pressure to vary in space and time, and look at the space and time dependent equation of state. However, our current approach is much simpler, and the experimental equation of state compares well with standard kinetic theory [7].

We measure the average density, horizontal and vertical temperatures, and radial distribution functions  $g(r)$  for three different constant pressures, for  $R$  from 1.5 – 5, and for  $\Gamma$  from 0–30. To prepare the system initially in the densest state, we increase  $\Gamma$  to 30 and then slowly lower the acceleration to zero. Then we alternate taking 1024 pictures with a small increase in  $\Gamma$  and a variable time delay (typically one second) until  $\Gamma = 30$ . Then we repeat the same process while decreasing  $\Gamma$  to zero. Typical data runs are shown in Fig. 2.

**Results:** The behavior of the system is quite different depending on the number of particles in the cell. If  $R$  is an integer then we observe a first-order hysteretic phase transition as we change  $\Gamma$ . Figure 2(a) shows a typical example for  $R = 4$ . Below  $\Gamma = 1$ , nothing happens — the temperatures are zero and the 2D volume fraction  $\nu$  is constant. As we increase  $\Gamma$  for  $1 < \Gamma < 8$ ,  $T_{VV}$  rises linearly. Initially,  $T_{HH} \simeq T_{VV}/2$ , but around  $\Gamma = 3$  the ratio drops and stays around 20%, as shown in Fig. 2(c).  $\nu$  remains nearly constant for  $\Gamma < 2$  and then falls linearly until  $\Gamma = 8$ . At  $\Gamma = 8$ , there is an abrupt change in all of the measured quantities.  $T_{VV}$  and  $T_{HH}$  rise by factors of 5 and 10 respectively, and the ratio reaches nearly 50%.

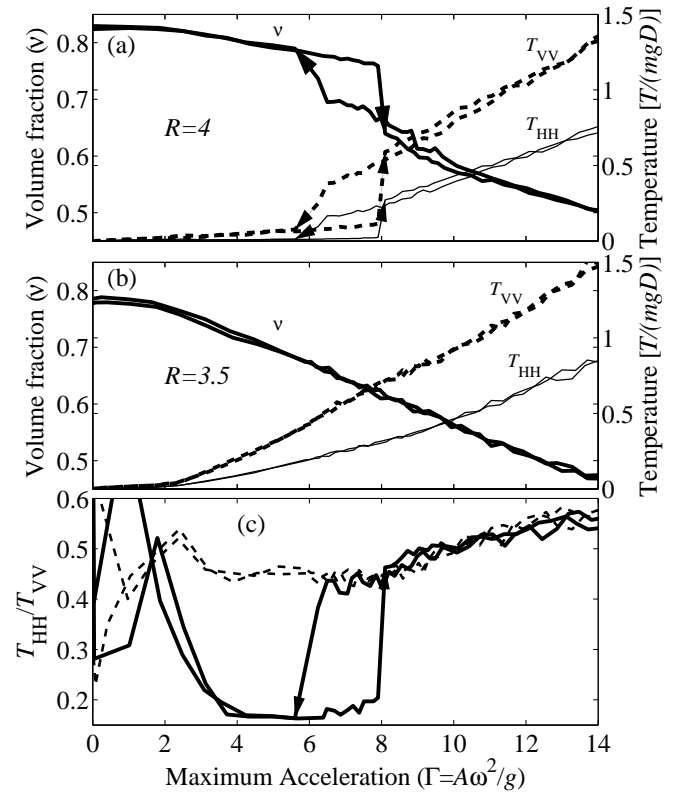


FIG. 2: (a)-(b) Plots of the volume fraction (thick) and average vertical (dashed) and horizontal (thin) temperatures as a function of increasing and decreasing  $\Gamma$  at 50 Hz, under isobaric conditions. (a) First-order phase transition for  $R = 4$ , showing a discontinuities in density and temperature as well as hysteresis. (b) For  $R = 3.5$ , the curves are smooth and non-hysteretic. (c) Plot of the horizontal to vertical temperature ratio for  $R = 3.5$  (dashed) and  $R = 4$  (solid).

$\nu$  drops by more than 15%. For  $\Gamma > 8$ ,  $T_{VV}$  and  $T_{HH}$  continue to rise, the ratio reaches 70% by  $\Gamma = 30$  (not shown), and  $\nu$  continues to drop. As  $\Gamma$  is lowered, the process is reversed, but the transition point shows 25% hysteresis, occurring at  $\Gamma = 6.1$ . The hysteresis is rate-dependent, and if the rate of change in  $\Gamma$  is increased by a factor of 100 the hysteresis is lost. Similar behavior is seen for  $R = 2, 3$ , and 5, although the size of the jumps decrease as  $R$  is decreased. For  $R = 3.5$  the situation is quite different, as shown in Fig. 2(b). All of the measured quantities change continuously as  $\Gamma$  is changed, and no hysteresis is observed. The ratio of  $T_{VV}$  to  $T_{HH}$  stays near 50% until  $\Gamma = 1$ . Similar behavior is seen for  $R = 1.5, 2.5$ , and 4.5.

$g(r)$  is shown in Fig. 1(d) for the  $R = 4$  states just before ( $\Gamma = 7.90$ ) and just after ( $\Gamma = 8.10$ ) the transition. While  $\Gamma$  only changes by 2.5%  $g(r)$  changes dramatically.  $g(r)$  for the gas state is typical for a hard sphere fluid near a freezing transition, including the broad peak just below  $r = 2D$  that is a precursor for freezing [8].  $g(r)$  for the crystalline state is typical of an expanded hard sphere

crystal at nonzero temperature, showing sharp peaks at  $r = D, 2D$ , and  $3D$ . There is a big peak at the next-nearest neighbor distance  $r = \sqrt{3}D$  with a splitting due to the fact that the average nearest neighbor distance is greater than  $D$  at a nonzero temperature.  $g(r)$  for  $R = 3.5$  at  $\Gamma = 8$  is not shown but is clearly fluid-like. Even at  $\Gamma = 3.88$  where the  $T_{VV}$  is equal to the crystal melting temperature,  $g(r)$  is intermediate between a crystal and fluid, with small peaks at integer separations, as shown in Fig. 1(d). In the image [Fig. 1(a)] crystalline regions can be seen, but there are gaps, holes, and dislocations. Information from  $g(r)$  is summarized in Fig. 3(b-c). In all of the crystallizing systems particles are excluded from a band at  $r = 1.5D \pm 0.1D$  and the average number of next nearest neighbors is near the maximum as shown in Fig. 3(b-c). The integer system is clearly in a crystalline state, but it is not clear if the half-integer system ever reaches a crystalline state. Another classic measure of melting is the Lindemann criterion [9], in which the average root-mean-squared particle displacements  $\gamma_m = \sqrt{\langle(\vec{r} - \langle\vec{r}\rangle)^2\rangle}/D > \gamma_c$ .  $\gamma_m$  is plotted against  $\Gamma$  in Fig. 3(a). We find a value of  $\gamma_c$  between 0.10–0.12 is consistent with all of the integer data. This also predicts that the half-integer systems freeze, but at a lower  $\Gamma$ , around 4 for  $R = 3.5$ . However, the predicted freezing temperatures for all data fall in a band between the crystal freezing and melting temperatures ( $T_{VV} = 0.1 - 0.6$ ). While the Lindemann criterion suggests that all of the systems freeze, it says nothing definitive about the structure of the solid and the radial distribution functions suggest that freezing is a continuous process for the half-integer systems. Recent work on elastic hard spheres using density-functional theory by Both and Hong [10] predicts a critical melting temperature determined by a constant  $\mu_0$ . From our melting and freezing temperature we find a range of  $\mu_0$  between 10–60 which is consistent with their findings.

To further exploit the analogy to thermodynamics, we have examined the average equation of state for this system. From  $T_{VV}$ , the average number density  $n = 4\nu/(\pi D^2)$ , and average pressure determined from the mass of the weight and half of the mass of the particles, we experimentally measure the compressibility factor  $\chi$  from the equation of state for this 2D granular fluid [11],  $P = nT_{VV}(1 + \chi(\nu))$ ;  $\chi = P/(nT_{VV}) - 1$ .  $\chi$  can be theoretically related to  $g(D)$ , through the virial for the pressure [12]. In an inelastic hard sphere fluid  $\chi(\nu) = \alpha\nu g(D; \nu) \equiv \alpha G(\nu)$ , where  $\alpha = (1 + e)$  and  $e$  is the coefficient of restitution. For an elastic hard sphere fluid  $e = 1$  and  $\alpha = 2$ . A number of forms for  $G$  are available in the literature (see [13] for a recent discussion). All are similar and we use the simple  $G_T$  developed by Torquato [14], which is an analytical fit to molecular dynamics simulation at high  $\nu$  and the Carnahan and Starling [15] geometric series approximation to the first few virial coefficients at low  $\nu$ .

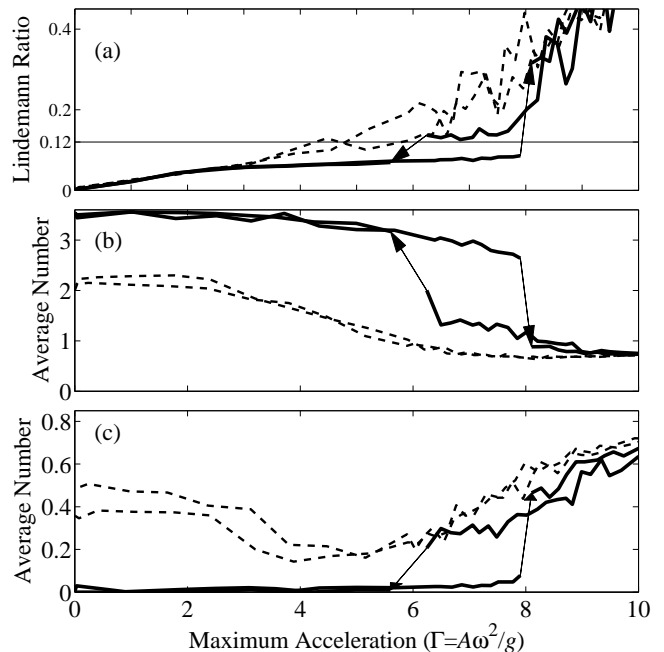


FIG. 3: Plots of the (a) Lindemann ratio and the average number of particles separated by (b)  $\sqrt{3}D \pm 0.1D$  and (c)  $1.5D \pm 0.1D$  versus  $\Gamma$  for  $R = 4$  (thick) and  $R = 3.5$  (dashed).

A plot of  $\chi$  versus volume fraction is shown in Fig. 4 for  $R = 3.5$  and 4.  $\chi$  remains  $\sim 10\%$  of  $2G_T$  up to  $\nu = 0.55$ ,  $R = 3.5$  and 4. Above 0.55 the half-integer system drops  $\sim 10\%$  below  $2G_T$ , but both  $\chi$  and its derivative are continuous functions of  $\nu$  up to  $\chi \simeq 200$ . Above this value,  $\Gamma$  is near 1, the temperatures are almost zero, and  $\chi$  strongly diverges. This behavior is expected, since our equation of state completely neglects the elastic forces between the particles. When the temperature goes to zero the weight is held up by elastic energy, not kinetic energy. However, the point at which this occurs is a very high density in which the pressure due to the density of the gas through the compressibility factor is 200 times the value of a dilute gas. The behavior above  $\nu = 0.6$  is quite different for the integer systems. As  $\nu$  increases there is a jump in both  $\chi$  and  $\nu$  signaling the phase transition. Above this volume fraction the system is in an expanded crystalline state like that shown in Fig. 1(b). The size and position of the gap depend on a number of parameters, including the history, number of rows, and confining pressure. In the crystalline state  $\chi$  increases until  $\Gamma$  is nearly one and the maximum recorded packing fraction is reached. At this point  $\chi$  diverges strongly as elastic forces become important. As with the half-integer case, the granular temperature must be very low and the density must be very close to the maximum before elastic consideration are important. This suggests that continuum theories based solely on kinetic considerations may have a range of applicability up to very high density and very low temperatures.

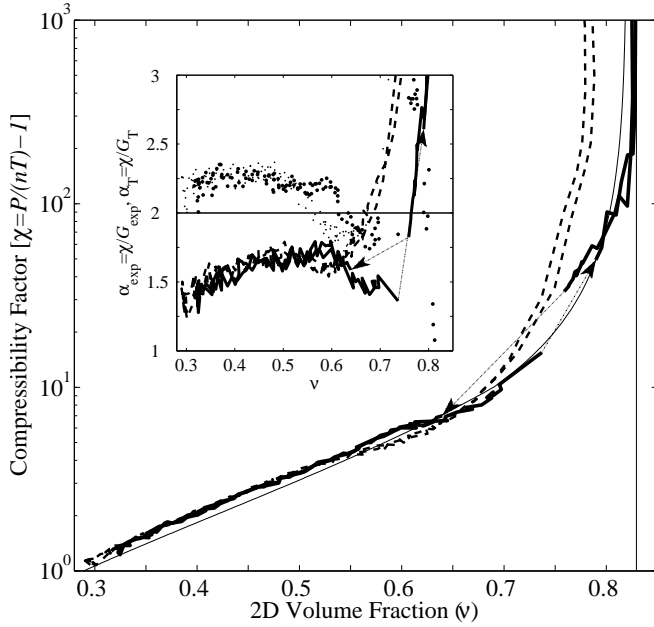


FIG. 4: Log-linear plot of the compressibility factor as a function of volume fraction, for  $R = 3.5$  (dashed),  $R = 4$  (thick), and  $2G_T$  (thin, see text). The dashed ( $R = 3.5$ ) and thick ( $R = 4$ ) curves in the inset show an experimental measurement of  $\alpha_{\text{exp}}$  (see text) as a function of volume fraction.  $\alpha = 2$  for elastic hard spheres. The large dots ( $R = 4$ ) and small dots ( $R = 3.5$ ) show  $\alpha_T$  using  $G_T$ .

To see the comparison between  $\chi$  and  $G_T$  more clearly, the inset of Fig. 4 plots  $\chi/G_T$  which should be 2 for elastic hard spheres and less for inelastic hard spheres. We can also measure  $G$  from the experimental  $g(D; \nu)$  and compare that to the experimental value of  $\chi$ .  $G_{\text{exp}}$  determined in this manner is only accurate for  $\nu < 0.8$ ; above this value the peak near  $D$  begins to split due to small imperfections in the crystal lattice, and the peak height stops growing. From  $G_{\text{exp}}$  we obtain a fully experimental measure of  $\alpha$ . The result is also shown on the inset of Fig. 4.  $\alpha_{\text{exp}}$  is consistent with our direct measures of  $e$  from particle tracking. We find values of  $e$  over a broad ranging from 0.3 to 1.3, and a general trend of lower values for higher collision velocities. Values of  $e > 1$  are possible since we cannot measure particle spin.

*Discussion:* The first-order phase transition seen in the integer number of rows is qualitatively different from that of an elastic hard sphere system. In such a system, just as in an ordinary gas, at the phase transition there is a discontinuous change in the density, but the temperature would be unchanged. This is a unique feature in granular systems since it suggests that there is the possibility of steady states in which two phases co-exist, but at different nonzero temperatures. States like these have been seen experimentally [16] and in simulation [17]. This co-

existence does not violate thermodynamics since a steady state is not the same as equilibrium, but it can have profound effects on continuum theories since it predicts discontinuities in the temperature field could exist in steady state without the need for energy or particle flow. That is, the system is mechanically stable since there are two states with the same pressure but different densities and internal energies. This would also interfere with the standard continuum assumption of near Maxwell-Boltzmann distributions, since near the gas/crystal border two different velocity distributions can co-exist. Any spatial average would include some of each distribution. So while the equation of state data suggests that theories based solely on kinetic consideration are applicable on either side of the phase transition, some modification will be needed to account for the discontinuities created by phase transitions.

This work was supported by The National Science Foundation, Math, Physical Sciences Department of Materials Research under the Faculty Early Career Development (CAREER) Program: DMR-0134837.

---

\* shattuck@ccny.cuny.edu; URL: <http://gibbs.engr.ccny.cuny.edu>

- [1] B. J. Alder and T. E. Wainwright, Phys. Rev. **127**, 359 (1962).
- [2] W. G. Hoover and F. H. Ree, J. Chem. Phys. **49**, 3609 (1968).
- [3] B. J. Alder, W. G. Hoover, and D. A. Young, J. Chem. Phys. **49**, 3688 (1968).
- [4] M. A. Rutgers, J. H. Dunsmuir, J. Z. Xue, W. B. Russel, and P. M. Chaikin, Phys. Rev. B **53**, 5043 (1996).
- [5] L. P. Kadanoff, Rev. Mod. Phys. **71**, 435 (1999).
- [6] D. Ruelle, J. Stat. Phys. **95**, 393 (1999).
- [7] J. T. Jenkins and M. W. Richman, Arch. Rat. Mech. Anal. **87**, 355 (1985).
- [8] T. M. Truskett, S. Torquato, S. Sastry, P. G. Debenedetti, and F. H. Stillinger, Phys. Rev. E **58**, 3083 (1998).
- [9] F. A. Lindemann, Phys. Z. **11**, 609 (1910).
- [10] J. A. Both and D. C. Hong, Phys. Rev. E **64**, 061105 (2001).
- [11] J. T. Jenkins and M. W. Richman, J. Fluid Mech. **192**, 313 (1988).
- [12] S. Chapman and T. G. Cowling, *The Mathematical Theory of Non-uniform Gases* (Cambridge University Press, London, 1970).
- [13] S. Luding, Phys. Rev. E **63**, 064220 (2001).
- [14] S. Torquato, Phys. Rev. E **51**, 3170 (1995).
- [15] N. F. Carnahan and K. E. Starling, J. Chem. Phys. **51**, 635 (1969).
- [16] J. S. Olafsen and J. S. Urbach, Phys. Rev. Lett. **81**, 4369 (1998).
- [17] B. Meerson, T. Pöschel, and Y. Bromberg, Phys. Rev. Lett. **91**, 024301 (2003).